19th Australasian Fluid Mechanics Conference
Melbourne, Australia
8-11 December 2014

Separation of Yawed Turbulent Flows over a Forward-Facing Ramp

D. F. Xie, H. M. Blackburn, and J. Sheridan

Department of Mechanical & Aerospace Engineering
Monash University, Victoria 3800, Australia

Abstract

Turbulent flows over a forward-facing ramp (FFR) were investigated using numerical methods. The present direct numerical simulations (DNS) were conducted under conditions with approaching wind directions from 0° to 45° in 15° increments in order to examine flow features and the effect of inflow yaw angle. A spatially developed turbulent inflow was generated by applying a recycle boundary condition. Reynolds number was 2000, based on ramp height and bulk mean velocity of the oncoming flow. The 45° ramp is assumed to be infinitely extended in the spanwise direction. DNS results show quantitative turbulence statistics and structures of boundary layer flows over a FFR.

Introduction

The study of a flow separating from the surface of a solid body, and characteristics of flow fields that develop as a result of the separation, are among the most fundamental and difficult problems of fluid dynamics. Flow separation is always expected at the salient edge of a bluff body, regardless of whether the boundary layer is laminar or turbulent. In the past there have been numerous studies [3, 12, 4, 10, 8, 11] dealing with separated-reattached flow over a forward-facing step (FFS). Despite the significant efforts made to understand such flows, very little effort has been directed towards a yawed flow over a forward-facing ramp (FFR). The proposed research is an investigation of turbulent flow over a FFR using direct numerical simulation. The engineering motivation of this work is to understand the topographical effects on underlying mechanism and detailed near-wall turbulent statistics, thus aiding the wind energy industry in establishing guidelines for turbine siting on escarpments. An equally important aspect is to investigate yaw effects on turbulence structure downstream of the flow separation zone.

Method

The governing equation used in the DNS is the incompressible Navier–Stokes equation without buoyancy terms is,

$$\nabla\cdot\mathbf{u}^*=0,\partial_t\mathbf{u}^*+(\mathbf{u}^*\cdot\nabla)\mathbf{u}^*=-\frac{1}{\rho}\nabla p^*+\nu\nabla^2\mathbf{u}^*+\mathbf{f}, \quad (1)$$

where $\mathbf{u}^*=[u,v,w]^T$ is the velocity vector, ρ is density, p^* is pressure, ν is kinematic viscosity and $\mathbf{f}$ is body force per unit mass of the flow. $\mathbf{f}$ is introduced so that average flow rate will be constant. By prescribing a spanwise $\mathbf{f}$ we could introduce a spanwise flow rate, thus achieving a yawed inflow.

With the non-dimensional case, new variables are achieved using the free-stream velocity U_∞, and escarpment height H:

$$\partial_t\mathbf{u}+(\mathbf{u}.\nabla)\mathbf{u}=-\nabla p+Re_H^{-1}\nabla^2\mathbf{u}+\mathbf{f}, \quad (2)$$

where Re_H=$U_\infty H/\nu$ is the Reynolds number, $p=p^*/\rho{U_\infty}^2$ is static pressure. The present DNS based on the spectral element method is carried out under conditions of constant Reynolds numbers based on the free stream bulk velocity, U_∞ and the height of the ramp, H. The ramp height is set to $1/5$ of the boundary layer thickness. The detailed computational conditions are indicated in Table 1, which includes the Reynolds number and domain information.

Re_H	2000
ramp slope	45°
domain size ($x\times y\times z$)	$62H\times 5H\times 4\pi H$
yaw angles(α)	0°, 15°, 30°, 45°

Table 1. Computational conditions.

The flow with a moderate yaw angle, i.e. $\beta\leqslant 45°$, over an escarpment is sketched in Figure 1. When $\mathbf{f}$ has a spanwise component, a considerable cross flow can develop over time, resulting in a skewed mean velocity profile. The boundary conditions for the velocity field are the non-slip conditions on the walls, and free-slip on the upper boundary. A special kind of boundary condition is prescribed at the inlet of the main simulation part to generate a spatially developed turbulent inflow, where the velocity field is duplicated at location $27H$ downstream of the inlet. This section was initialized from a turbulent open channel flow with the same size, known as the development part. It is a variation of the method for generation of turbulent inflows proposed by [6], here is referred to as recycled boundary condition. Periodicity is applied in the spanwise direction. Domain length and width are tested using two-point correlations, the correlation curves fall off towards zero indicating convergence is achieved. Therefore, current dimensions are considered to be adequate for the objectives of the present work.

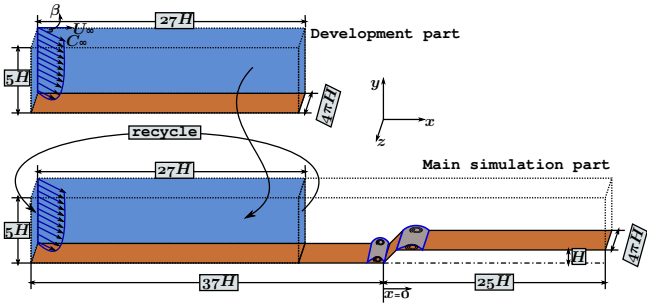

Figure 1. Ramp coordinates system x,y,z

Results

The Yawed Turbulent Boundary Layer ahead of the Ramp

In theory, the inflow generation method of [6] should also work by adding a yaw angle. However, prior to the study of flow separation we need to validate the outcome of the simulations in the recycled region.

One validation can be achieved by comparing the velocity profiles at various yaw angles. Reynolds number were kept constant at $Re_H = 2000$ (or approximately 480 based on δ and u_τ). As the recycled region could be considered as a open channel flow. This enables comparison to the DNS results [7] at $Re_\tau = 590$. Figure 2 shows the comparison of mean velocity profiles obtained from various yaw angle simulations within the recycled region. The current simulations and channel flow data are seen to be in quite good agreement. It should be noted that the yawed velocity profiles in the outer region are relatively lower than the non-yawed case, indicating yawed simulations are slightly under-resolved.

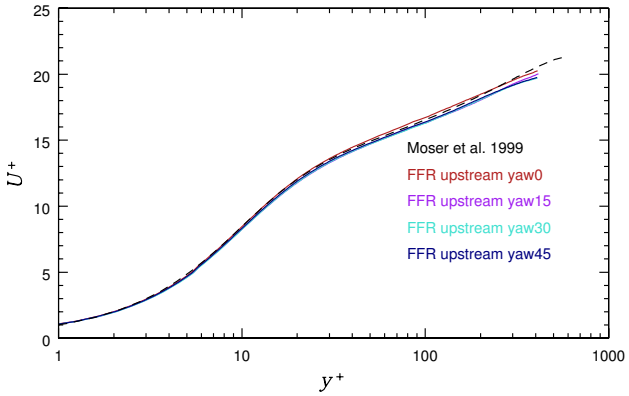

Figure 2. Mean velocity profiles at different yaw angles compared with channel flow results of [7]

In order to monitor the convergence of simulations, fluctuating energy budget equation for a constant-viscosity fluid is introduced,

$$\overbrace{U_j \frac{\partial Q_T}{\partial x_j}}^{1} = \overbrace{-\frac{\partial \overline{u_i' u_i' u_j'}}{\partial x_j}}^{2} \overbrace{-\frac{\partial \overline{p' u_j'}}{\partial x_j}}^{3} \overbrace{+2\frac{\partial N \overline{s_{ij}' u_i'}}{\partial x_j}}^{4} = \underbrace{-2N\overline{s_{ij}' s_{ij}'}}_{5} \underbrace{-\overline{u_i' u_j'} S_{ij}}_{6} \tag{3}$$

Where, sum of the above terms of Newtonian fluids equations zero in equilibrium stage.

Figure 3 shows the vertical profile of terms in the turbulent kinetic energy budget equation (3) for each yawed flow in the recycled region. It can be seen that the sum of terms oscillates around zero in each case indicting that the simulations have reached statistical equilibrium.

Main Flow and Reattachment

It is believed that flow features, such as speed-up and separation, are influenced by the approaching flow direction. Therefore set up a desired yaw angle is critical for further investigations of such flows. Figure 4 indicates the yaw angle along streamwise axis which includes recycled upstream, ramp and downstream regions. Yaw angle were obtained by tangential wall shear stresses. As seen, the proposed yaw angle were accomplished quite successfully. When the flow hits the ramp, flow angle deviates significantly due to separation and reattachment. Yaw angle relaxes in few step heights downstream at a lower level as streamwise velocity has an increases of 25% which is expected due to the blockage ratio of 0.2 downstream.

One of the key features of flow over complex terrain is local "speed-up". Non-dimensional, it is expressed as the fractional

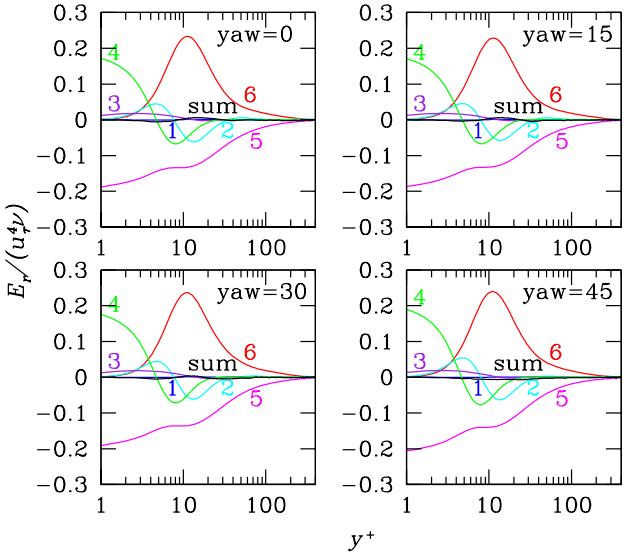

Figure 3. Normalized terms in the fluctuating energy budget for Newtonian fluid at various yaw angles from 0° to 45°, where ① mean flow advection; ② turbulent transport; ③ pressure-gradient work; ④ mean viscous transport; ⑤ mean viscosity dissipation; ⑥ production; [sum] of above.

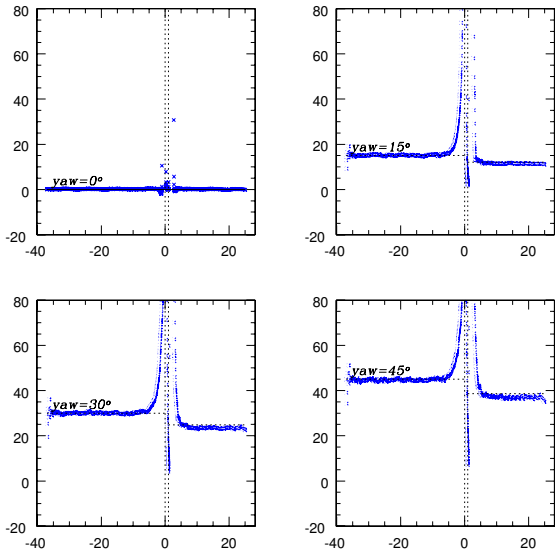

Figure 4. Wall shear stress angle chart along streamwise axis.

speed-up ratio, ΔS, which is given by

$$[\Delta u(z)L]/[u_0(2L)H], \tag{4}$$

which uses the same calculation as that found in Bitsuamlak's review paper [2]. In these expressions H represents the height of the ramp, L represents the horizontal distance from the crest to where the ground elevation is half the height of the ramp, $\Delta u(z)$ represents increase in velocity, i.e., $u(z) - u_0(z)$ at height z above the local ramp surface, $u_0(2L)$ represent upstream reference velocity at the height $2L$ above the ground respectively, similarly $u_0(z)$ represent upstream reference velocity at height z above the ground respectively, Figure 5(a).

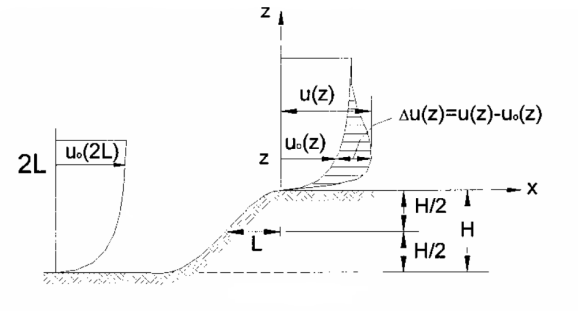

(a)

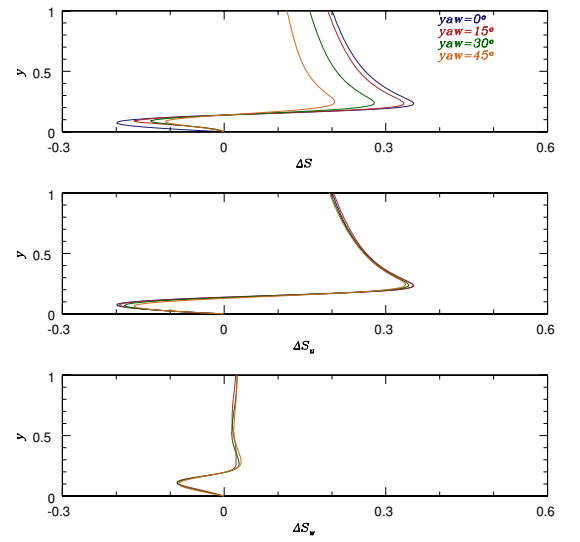

(b)

Figure 5. (a) definitions of parameters for calculations of normalized speed-up ratio; (b) dimensionless total velocity speed-up factor (ΔS), streamwise (ΔS_u) and spanwise (ΔS_w) at $1.5H$ downstream with yaw angle 0°, 15°, 30° and 45°.

Figure 5(b) represents normalized speed-up values at $1.5H$ after the top edge. By comparing four different yawed flows, we found that mean velocity of all cases have reverse flow regions, i.e. $\Delta S < 0$, indicating re-circulation zones. We also found that speed-up value decreases as yaw angle increases, therefore flows without yaw angle give maximum speed-up ratio near the wall. On the other hand, speed-up ratios of various yaw angle flows on streamwise and spanwise are almost identical, indicating sweep-independence. Note that not only the velocity component normal to the edge is accelerated, a minor speed-up on the spanwise component is also observed, which is contradictory to the conclusion made by Baker [1] that speed-up only occurs in the streamwise direction.

The difficulty with investigation of FFR arises from the existence of flow separations regions, where high turbulence exists. It is well-known that the separation regions occur in front of and on the edge in the FFS flow. The present DNS obviously show the same characteristics. In this study separation and reattachment points are almost fixed in the first bubble for each yawed flow, which were arisen from the adverse pressure gradient caused by the blockage of flow at the ramp face. [12] reviewed the past work on the separations caused by a FFS, and indicating that the second recirculation length is somewhere between $1.4h$ to $5.0h$. In current work, the second bubble is also within this range for each yaw angles. The reattachment point can be well represented by the distributions of friction coefficients, Figure 6, which gives a similar structual distribution of friction coefficients in comparison with previous studies [4]. On the other hand, different distribution of friction coefficients are found on the ramp when yaw angle applies. This is because the fluctuating velocity impinging toward the step is mainly reflected in the spanwise direction and the second bubble is highly affected by upstream condition. The downstream reattachment length at different yaw angles can be found in Table 2. The longest reattachment after the ramp is obtained in the case of the highest yaw angle.

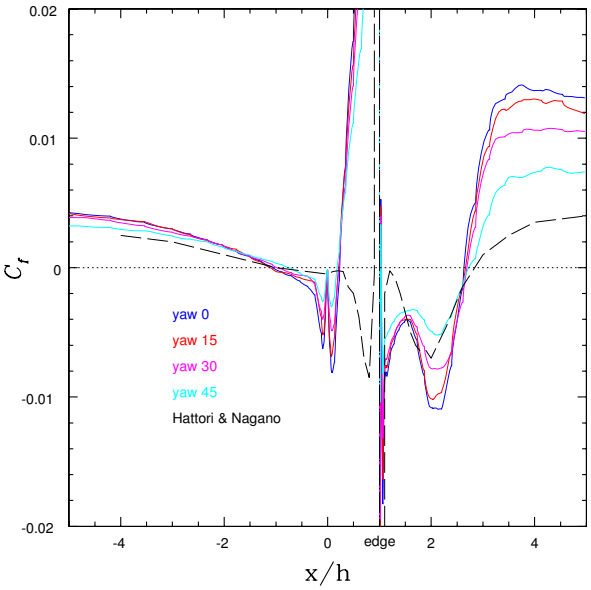

Figure 6. Distribution of friction coefficients with yaw angle 0°, 15°, 30° and 45°.

Yaw angle	Downstream reattachment lengths
0°	$1.62H$
15°	$1.63H$
30°	$1.65H$
45°	$1.68H$

Table 2. Downstream reattachment length along streamwise with various yaw angles.

Turbulence Statistics

The instantaneous velocity fields have been analyzed to educe turbulence coherent structures and study their dynamics. Jeong [5] suggests vortices are well-represented by connected regions where the second largest eigenvalue(λ_2) of the tensor $S_{ik}S_{kj} + \Omega_{ik}\Omega_{kj}$ is negative, here $S_{ij} \equiv (u_{i,j} + u_{j,i})/2$ and $\Omega \equiv (u_{i,j} - u_{j,i})/2$ are the symmetric and antisymmetric parts of the velocity gradient tensor $u_{i,j} \equiv \partial u_i/\partial x_j$. The lateral view of isosurfaces of $\lambda_2 = -50$ for various yaw angles reveals collections of vortices near-wall structure (Figure 7). Clearly, the dominant vortices are aligned predominantly with incoming flow ($\hat{x}$). Most of λ_2 regions occur around the ramp, which are known as the low-pressure regions. It is remarkable that yawed flow vortices become more intense than zero sweep. A possible cause for the observed increase in vortices in near wall region for high yaw angle is the fact that vortices which are not aligned with the homogeneous direction experience an extensional strain along

their axis. Note that the $-\lambda_2$ tend to incline at a positive angle respect to the x-direction ($x-y$ plane, not shown). We can also see some roller or rib structures. Though hairpin vortex line bundles do occur, the hairpin vortex are yet to confirm.

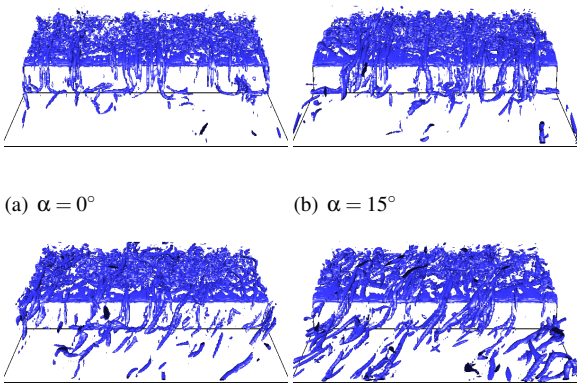

(a) $\alpha = 0^\circ$ (b) $\alpha = 15^\circ$

(c) $\alpha = 30^\circ$ (d) $\alpha = 45^\circ$

Figure 7. Lateral view of the isosurfaces of $\lambda_2 = -50$ with various yaw angles

The behavior of flow over a surface associated with separation usually results in a pattern of lines emanating from critical points where the shear stress, τ, are identically zero [9]. Figure 8 shows the u-contours and streamlines at $y = 1.05H$. There are few streamlines from upstream that joins this line, which indicates the three-dimensional flow separation feature. Inside the recirculation region, there are number of critical points occur in the non-yawed case. Among these critical points, node and saddle are most obvious. Surface bifurcation lines are visualized in all yawed case, which is an evidence of present of the longitudinal vortices. Note that all the critical points occurs at the zero u velocity.

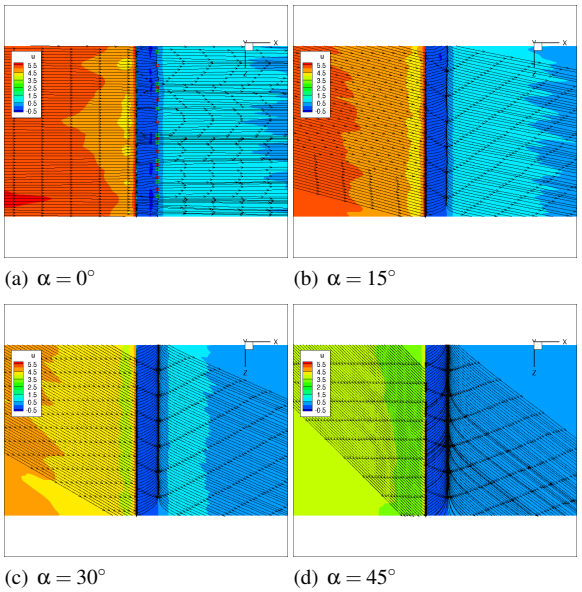

(a) $\alpha = 0^\circ$ (b) $\alpha = 15^\circ$

(c) $\alpha = 30^\circ$ (d) $\alpha = 45^\circ$

Figure 8. u-contours and streamlines at $y = 1.05H$

Conclusion

Direct numerical simulations of turbulent boundary layer flow over a FFR are performed to investigate the effect of the FFR at various yaw angles. Current DNS studies show detailed turbulent motion around the ramp with the influence of yaw angle. In particular, it is found that the separation-reattachment region upstream is little affected by the yaw effect. However, the flow fields in the downstream recirculation region are highly depend on the yaw angle. Further investigation with larger Reynolds number is spectral vanishing viscosity (SVV) method.

References

[1] Baker, C.J, The determination of topographical exposure factors for railway embankments, *Journal of Wind Engineering and Industrial Aerodynamics*, **21**, 1985, 89–99.

[2] Bitsuamlak, G.T., Stathopoulos T. and Bédard C., Numerical Evaluation of Wind Flow over Complex Terrain: Review, *Journal of Aerospace Engineering*, **17**, 2004, 135–145.

[3] Camussi, R., Felli, M., Pereira, F., Aloisio, G. and Di Marco, A., Statistical properties of wall pressure fluctuations over a forward-facing step, *Physics of Fluids*, **20**, 2008, 075113.

[4] Hirofumi Hattori and Yasutaka Nagano, Investigation of turbulent boundary layer over forward-facing step via direct numerical simulation, *International Journal of Heat and Fluid Flow*, **31**, 2010, 284–294.

[5] Jeong, Jinhee and Hussain, F., On the identification of a vortex, *Journal of Fluid Mechanics*, **285**, 1995, 69–94.

[6] Lund, T.S., Wu, Xiaohua and Squires, K.D., Generation of Turbulent Inflow Data for Spatially-developing Boundary Layer Simulations, *J. Comput. Phys.*, **140**, 1998, 233–258.

[7] Moser, R.D., Kim, J. and Mansour, N.N., Direct numerical simulation of turbulent channel flow up to $Re_\tau = 590$, *Physics of Fluids*, **11**, 1999, S1070-6631(99)02204-7.

[8] Pearson, D.S., Goulart, P.J. and Ganapathisubramani, B., Turbulent separation upstream of forward-facing step, *Journal of Fluid Mechanics*, **724**, 2013, 284–304.

[9] Perry, A.E. and Chong, M.S., Topology of flow patterns in vortex motions and turbulence, *Applied Scientific Research*, **53**, 1994, 357–374.

[10] Huiying Ren and Yanhua Wu, Turbulent boundary layers over smooth and rough forward-facing steps, *Physics of Fluids*, **23**, 2011, 045102.

[11] Scheit, C., Esmaeili, A. and Becker, S., Direct numerical simulation of flow over a forward-facing step - flow structure and aeroacoustic source regions, *International Journal of Heat and Fluid Flow*, **43**, 2013, 184–193.

[12] Sherry, M., Lo Jacono, D. and Sheridan, J., An experimental investigation of the recirculation zone formed downstream of a forward facing step, *Journal of Wind Engineering and Industrial Aerodynamics*, **98**, 2010, 888–894.